

CHAPTER 3  
METHODOLOGY

3.1 Program Information

Based on steady-state continuous flow modeling (McCreanor, 1994) and investigation of other commercially available software packages, the United States Geological Survey's Saturated-Unsaturated Flow and Transport model (SUTRA) was chosen to continue modeling the recirculating landfill. SUTRA uses a two-dimensional hybrid finite element and integrated finite difference method to approximate the governing equations of flow and transport. SUTRA is capable of performing steady-state and nonsteady-state simulations.

The fluid mass balance governing equation used in SUTRA is:

$$\left( S_w \rho S_{op} + \varepsilon \rho \frac{\partial S_w}{\partial p} \right) \frac{\partial p}{\partial t} + \left( \varepsilon S_w \frac{\partial \rho}{\partial U} \right) \frac{\partial U}{\partial t} - \nabla \cdot \left[ \left( \frac{k k_r \rho}{\mu} \right) \cdot (\nabla p - \rho \underline{g}) \right] = Q_p \quad (3.1.1)$$

where:

|                 |   |  |
|-----------------|---|--|
| $S_w$           | = | water saturation, dimensionless  |
| $\rho$          | = | liquid density, $ML^{-3}$  |
| $S_{op}$        | = | specific pressure storativity, $LT^2M^{-1}$                                |
| $\varepsilon$   | = | porosity, dimensionless  |
| $p$             | = | pressure, $ML^2T^{-2}$   |
| $t$             | = | time, T  |
| $U$             | = | solute concentration or temperature, $M_{solute}/M_{fluid}$ or $^{\circ}C$ |
| $\underline{k}$ | = | solid matrix permeability, $L^2$   |
| $k_r$           | = | relative permeability, dimensionless                                       |
| $\mu$           | = | viscosity, $ML^{-1}T^{-1}$   |
| $\underline{g}$ | = | gravity acceleration vector, $LT^{-2}$                                     |
| $Q_p$           | = | fluid mass source, $ML^{-3}T^{-1}$   |

The physical significance of the terms in Equation 3.1.1 are explained in Table 3.1.1.

Table 3.1.1. Physical Significance of Terms in the SUTRA Governing Equation 3.1.1.

| Term* | Physical Significance   |
|-------|---|
| 1     | Changes in stored liquid due to changes in saturation or hydrostatic pressure |
| 2     | Changes in fluid density due to concentration or temperature changes          |
| 3     | Movement due to pressure and density changes                                  |
| 4     | Fluid mass sources  |

\*Terms are counted from left to right in Equation 3.1.1..

Terms one, three, and four are the only terms of importance in the simulations documented here. Term two has no effect due to the fact that there are no changes in temperature or solute concentration. Term one, specifically the specific storativity, had a large effect on simulation results and the accuracy of the fluid mass balance.

A general form of Darcy's Law (Equation 3.1.2) is used to simulate the mechanisms of pressure and density driving forces for flow:

$$v = \frac{(K k_r)}{(e S_w \mu)} * (\nabla P - \rho g) \quad (3.1.2)$$

where:

|                |   |   |
|----------------|---|---|
| v              | = | average fluid velocity, LT <sup>-1</sup>    |
| K              | = | solid matrix permeability, L <sup>2</sup>   |
| k <sub>r</sub> | = | relative permeability, dimensionless        |
| g              | = | gravity, LT <sup>-2</sup>                   |
| P              | = | pressure, ML <sup>2</sup> T <sup>-2</sup>   |
| ρ              | = | density, ML <sup>-3</sup>                   |
| e              | = | porosity, dimensionless                     |
| S <sub>w</sub> | = | water saturation, dimensionless             |
| μ              | = | viscosity, ML <sup>-1</sup> T <sup>-1</sup> |

SUTRA is equipped with subprogramming to model the interrelationship of saturation, capillary/suction pressure, and relative permeability for unsaturated flow modeling. SUTRA can model up to ten regions with different unsaturated properties. The unsaturated relationships are input as either Brooks and Corey equations, van Genuchten equations, or in a tabular format.

The basis of the SUTRA simulation is a mesh of nodes in Cartesian coordinates which are then connected to form quadrilateral elements. The construction of this mesh entails numbering each node and defining its location in Cartesian co-ordinates. Then each element is numbered and the four nodes which define its boundaries are indicated. An example of a simple finite element mesh is shown in Figure 3.1.1, element numbers are bold and node numbers are italicized. In this mesh, element two, the shaded box, would be bounded by nodes two, three, seven, and six and would have a bandwidth of five ( $7 - 2 = 5$ ). In this simple mesh, the bandwidth will be the same for each element. However, this is not always true. In addition to location, each node is assigned a porosity, a thickness, and a region number. The thickness is used in areal simulations to define changes in the aquifer thickness and can be used in cross-sectional simulations to simulate radial coordinates/flow. The region number defines which unsaturated region the particular node belongs to and identifies the unsaturated relationships to be used at this node.

The properties assigned on an elementwise basis are the maximum and minimum intrinsic permeability, the angle of anisotropy, the maximum and minimum longitudinal dispersivities, the maximum and minimum transverse dispersivities, and region numbers. The region numbers define to which unsaturated flow region each element belongs.

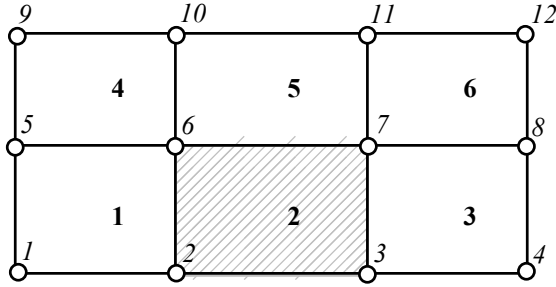


Figure 3.1.1. Diagram of a finite element mesh (elements numbers are bold, node numbers are italic).

The fluid properties include compressibility, specific heat, diffusivity, density at base concentration or temperature, base solute concentration or temperature, coefficient for density change, and viscosity. The solid matrix properties input are compressibility, specific heat, diffusivity, and density.

Additionally, SUTRA requires the input of the type of flow (saturated or unsaturated), the time basis of the simulation (steady state or transient), temporal discretization information related to the total length of the simulation, the maximum size of time steps within the simulation, the maximum number of iterations within a time step, and the iteration convergence criterion for the pressure and transport solutions.

SUTRA output includes a nodewise printout of pressures and concentrations at the first and last time steps as well as other time steps as specified by the output increment. If prompted, SUTRA will also provide printouts of nodewise and/or element-wise inputs, contourable plots of pressure and/or concentration and temperature, element-wise fluid velocities, and the overall fluid mass budget.

After permeability, the most important aspect of the waste is the modeling of its

unsaturated properties. The unsaturated flow properties of waste have been documented by Straub and Lynch (1982), Noble and Arnold (1991), Korfiatis et al. (1984), and Al-Yousfi (1994). These researchers used power, exponential, and statistically derived equations to model the relationships between percent saturation, suction head or capillary pressure, and relative hydraulic conductivity (see Section 2.3.2). The power equations proposed by Korfiatis et al. (1984) with  $b=4$ ,  $B=11$  and  $h_s=-609.2$  kPa were used to model the unsaturated characteristics of the waste matrix.

In order to improve simulation of the landfill scenario, the following changes were made to the SUTRA code:

- the bandwidth limit was expanded by an order of magnitude,
- power, exponential, linear and PITTLEACH equations for the interrelationship of saturation, pressure, and hydraulic conductivity were added,
- the boundary conditions were modified to include a pressure and/or saturation dependent fluid removal term,
- the output files were re-configured for importation to SURFER and database programs which will aid in analysis and interpretation of results, and
- the entire code was compiled in UNIX-Fortran in order to decrease modeling time.

The two most commonly used recirculation devices, the horizontal trench and the vertical recharge well were modeled. The impact of the following was considered:

- waste and daily/intermediate cover permeability on leachate hydrodynamics,
- effects of waste heterogeneities on leachate routing, and
- dynamic considerations related to recirculation volumetric loadings due to input device clogging or variable operational approaches on leachate hydrodynamics.

These goals were achieved through three primary modeling programs:

- conceptual modeling,
- stochastic modeling, and
- verificational modeling.

Each of these programs had its own modeling subsets, methodologies, and requirements as discussed below.

### 3.2 Conceptual Modeling

The conceptual modeling program was used to analyze the effect of leachate reapplication technique, waste permeability, daily cover, application rate, and frequency of leachate input. Waste permeabilities of  $10^{-3}$ ,  $10^{-4}$ , and  $10^{-5}$  cm/s were modeled for both the horizontal trench and vertical well simulations. Two leachate operational strategies were evaluated in order to assess the effect of operational frequency, continuous flow and 8 hr on/16 hr off.

The effect of daily cover was assessed using a low permeability ( $10^{-5}$  cm/s) material placed at 5 m vertical intervals with a 50-cm thickness. Leachate was applied intermittently, 8 hr on/16 hr off, via the horizontal trench at average daily rates of 2, 4, and 8 m<sup>3</sup>/m of trench.

The waste mass was also modeled as homogeneous and anisotropic with the vertical permeability modeled as either  $10^{-3}$  or  $10^{-4}$  cm/s. The horizontal permeability was modeled as one order of magnitude lower and higher than the vertical permeability. Leachate was again applied intermittently via the horizontal trench. Application rates are discussed in more detail below and in the results section.



### 3.2.1 Horizontal Trench

Modeling of the horizontal trench was conducted using leachate loading rates of 2, 4, and 8 m<sup>3</sup>/day/m of trench. The minimum flow rate (2 m<sup>3</sup>/day/m) was based on reported full-scale flow rates. The horizontal trench, 2 m wide by 1 m deep, was simulated in cross section as shown in Figure 3.2.1.

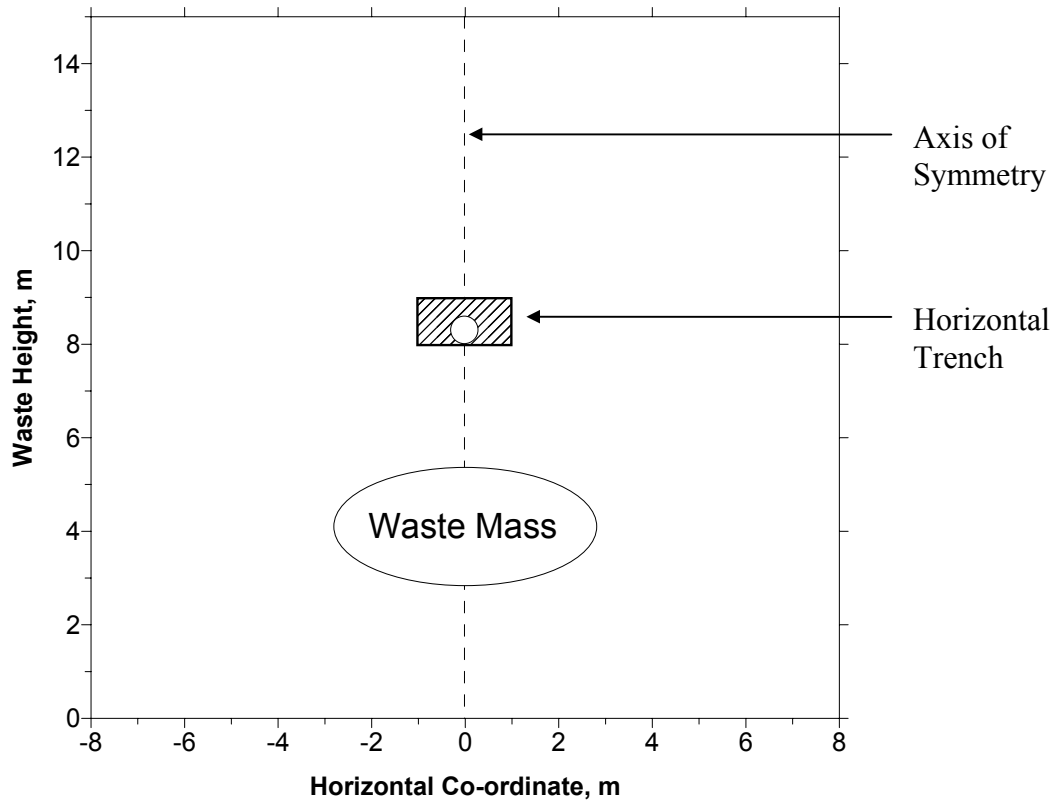


Figure 3.2.1. Cross-section of the waste matrix simulated for the horizontal trench .

Dimensional symmetry enabled the trench to be simulated in half-width which significantly reduced simulation times. The trench fill material had a porosity of 0.3 and a permeability of  $10^{-1}$  cm/s.

The leachate collection system (LCS) was modeled using typical characteristics for a sand and gravel media. A 50-cm layer of sand was placed on top of a 5-m layer of gravel. The gravel layer was oversized in order to act as storage for arriving leachate. An effort to model the behavior of the LCS was attempted however, this increased the model complexity significantly and caused stability problems.

#### 3.2.1.1 Horizontal Trench Model Calibration

Model calibration was initially performed by inspecting fluid mass balances produced by SUTRA. It was assumed that if these results indicated conservation of mass then the modeling assumptions were acceptable. It was found, however, during result analysis that the mass balances produced by SUTRA were not accurate. The software package Surfer® (Golden Software, Inc., Golden, CO.) was used to generate saturation iso-clines from SUTRA output. A Surfer® sub-function was then used to calculate the volume of liquid these iso-clines represent. It was found that the generated iso-clines did not represent the amount of liquid injected. Attention was immediately given to both spatial and temporal discretization, both of which had been previously calibrated and verified through visual inspection of saturation iso-clines and a node by node comparison of pressures and

saturations. Neither mitigated the mass balance problem. The time factor ,  $T_v$ , (Equation 3.2.1) is commonly used as a stability check for saturated hydraulic and geotechnical simulations. An analysis of model stability based on  $T_v$  was conducted.

$$T_v = \frac{c_v \cdot t}{H_{dr}^2} \quad (3.2.1)$$

where:

|          |   |  |
|----------|---|--|
| $T_v$    | = | time factor, unitless                      |
| $c_v$    | = | coefficient of consolidation, $L^2T^{-1}$  |
| $t$      | = | time step, T                               |
| $H_{dr}$ | = | drainage length or maximum element size, L |

A time factor of 0.05 is commonly used for simulation stability. The time step,  $t$ , and element size,  $H_{dr}$ , are straight forward concepts. The coefficient of consolidation,  $c_v$ , is more complex, as can be seen in Equations 3.2.2a, b, c.

$$c_v = \frac{k}{\gamma_w \cdot m_v} \quad (3.2.2a)$$

$$m_v = \frac{a_v}{1 + e_o} \quad (3.2.2b)$$

$$a_v = \frac{\partial e}{\partial (\Delta p')} \quad (3.2.2c)$$

where:

|             |   |  |
|-------------|---|--|
| $c_v$       | = | coefficient of consolidation, $L^2T^{-1}$          |
| $k$         | = | hydraulic conductivity, $LT^{-1}$                  |
| $\gamma_w$  | = | unit weight of water, $ML^{-3}$                    |
| $m_v$       | = | coefficient of volume compressibility, $L^2M^{-1}$ |
| $a_v$       | = | coefficient of compressibility, $L^2TM^{-1}$       |
| $e$         | = | void ratio, unitless                               |
| $\Delta p'$ | = | effective pressure, $ML^{-2}T^{-1}$                |
| $e_0$       | = | initial void ratio, unitless                       |

The time factor,  $T_v$ , is then a function of the time step and element size as well as permeability, compressibility, and the void ratio (or porosity). Additionally, the coefficient of compressibility,  $a_v$ , is constant only over a narrow range of pressure increase since  $\partial/\partial(\Delta p')$  is not a linear function.

The compressibility of the fluid and solid matrix had both been initially set to zero based upon the following statement found on page in the SUTRA manual (Voss, 1984):

“While the concepts upon which specific pressure storativity,  $S_{op}$ , is based, do not exactly hold for unsaturated media, the error introduced by summing the storativity term with the term involving  $(\partial S_w/\partial p)$  is insignificant as  $\partial S_w/\partial p \gg \gg S_{op}$ ” pp. 34

The thought had been that this would completely eliminate the specific storativity effects from the simulation results. Specific storativity refers to the phenomenon by which pore spaces are deformed and water is compressed due to effective stress (pore water pressure).

The combination of these two phenomena results in storage in excess of the measured porosity. Changes in local hydrostatic pressure (in saturated regions) then results in the storage or release of liquid.

Leachate injection systems, however, are atypical unsaturated flow problems from many aspects. The most fundamental and profound difference from a modeling perspective is that these systems involve the injection (under pressure) of large amounts of liquid into an unsaturated environment resulting in a pressurized, saturated bulb with unsaturated regions at the boundaries. This results in a highly complex system which must account for the release of liquid stored under pressure in pore spaces into unsaturated pores.

Based on the concepts mentioned above, a sensitivity analysis was performed on the solid matrix coefficient of compressibility factor. The liquid matrix compressibility was set to  $4.47 \times 10^{-10} \text{ m} \cdot \text{s}^2/\text{kg}$ . The assumption was that compressibilities resulting in  $T_v=0.05$  would provide close to accurate simulation results where accuracy was based upon the examination of the mass balance. This assumption did not prove to be the case as can be seen in Figure 3.2.2.

Ultimately, it was determined that the compressibility had to be set to  $1/100^{\text{th}}$  of the hydraulic conductivity in order to achieve reasonable mass balances. This ratio corresponds to  $T_v=5.8$  for a 10-minute time step or  $T_v=2.9$  for a 5-minute time step. Ultimately, a 10-minute time step was used, as this significantly decreased simulation time while impacting mass balance accuracy only slightly. A spatial discretization of 25 cm was used throughout the waste matrix.

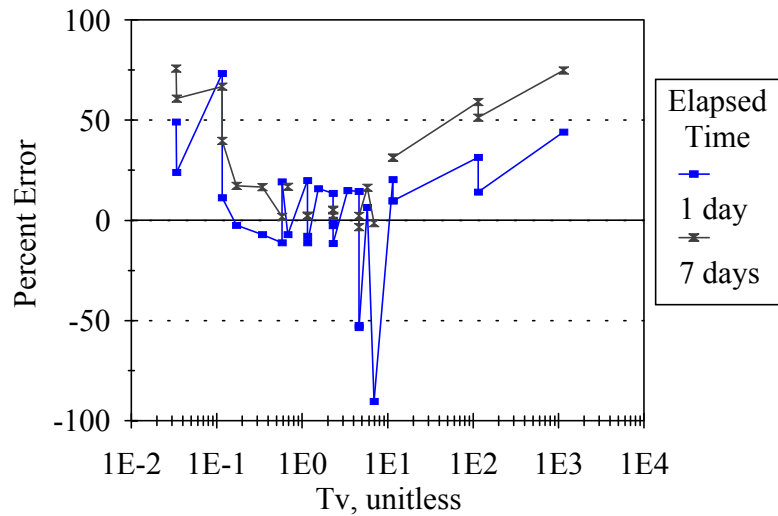


Figure 3.2.2. Percent error in mass balance versus time factor for horizontal trench simulations.

### 3.2.2 Daily Cover Material Effects

The impact of daily cover materials was assessed using the horizontal trench recirculating leachate intermittently (8 hr on/16 hr off) at average daily rates of 2, 4, and 8 m<sup>3</sup>/m of trench. The waste modeled in these simulations had uniform permeabilities of 10<sup>-3</sup> or 10<sup>-4</sup> cm/s while the cover material had permeabilities ranging from 10<sup>-2</sup> to 10<sup>-5</sup> cm/s, and a thickness of 0.4 m. The daily cover layer was modeled as both continuous and as breached with 1-m gaps created in two locations at each cover material level, Figure 3.2.3.

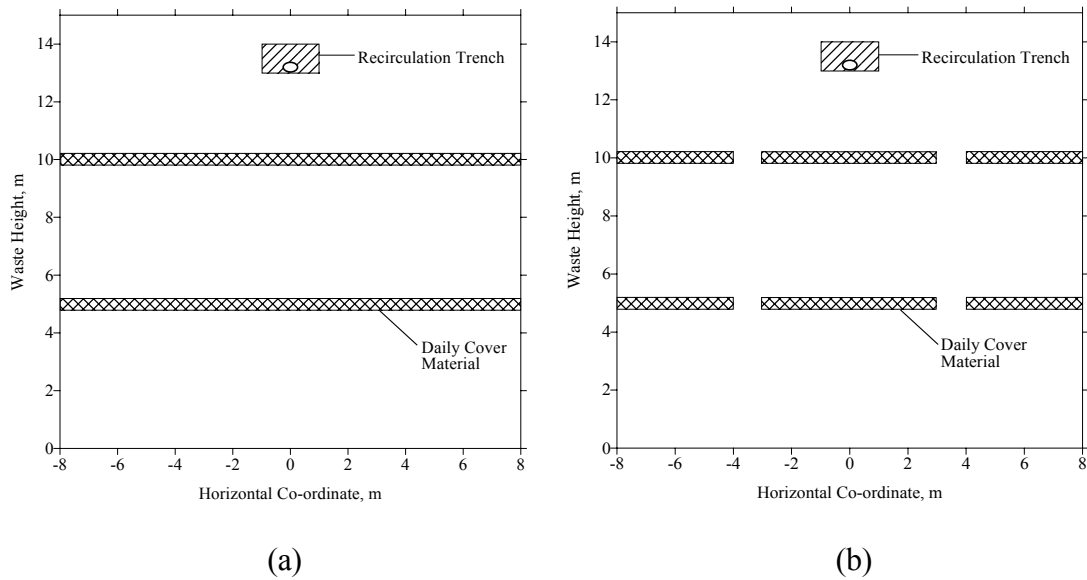


Figure 3.2.3. Diagram of continuous (a) and breached (b) daily cover layers simulated.

### 3.2.3 Anisotropic Waste Mass

The effect of homogeneous anisotropic waste mass on the behavior of the horizontal trench was also studied. The exact same simulation technique described above for the horizontal trench was used except for the following changes. The maximum and minimum permeabilities were assumed to occur in the vertical and horizontal directions. The vertical permeabilities were modeled as either  $10^{-3}$  or  $10^{-4}$  cm/s while the horizontal permeability was varied one order of magnitude above and below these values. Finally, the compressibility again required calibration and was “dialed” in for each combination of vertical and horizontal permeabilities.

### 3.2.4. Vertical Well

Modeling of the vertical well was conducted using a radial co-ordinate system with a well diameter of 1.2 m. Flow rates of 5, 10, 15, 20, 30, and 60 m<sup>3</sup>/day were used for constant injection cases. Intermittent injection (8 hr on/16 hr off) was modeled at average rates of 5, 10, and 20 m<sup>3</sup>/day. The lowest flow rate was based on reported operational rates.

The effect of increasing fluid pressure with depth within the well was simulated using "stepped" nodal flows as shown in Figure 3.2.4.

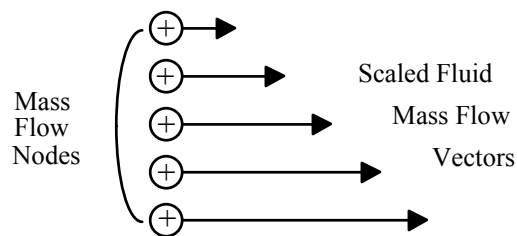


Figure 3.2.4. Diagram of flux nodes which simulate the vertical well.

The intent of this stepped approach was to simulate the effect of the variation of discharge velocities with depth along the well. The individual nodal flows were calculated using an incremental flow unit as shown in Equation 3.2.3.



$$q' = \frac{q}{\sum_{i=1}^n i} \quad (3.2.3)$$

where:

$$\begin{aligned} q' &= \text{incremental flow unit, MT}^{-1} \\ q &= \text{total flow to well, MT}^{-1} \\ n &= \text{the number of nodes used to simulate the well flow} \\ i &= \text{integer} \end{aligned}$$

The well discharge nodes were then numbered from the top down, beginning with one.

The individual nodal discharges were calculated using Equation 3.2.4.

$$q_m = m \cdot q' \quad (3.2.4)$$

where:

$$\begin{aligned} q_m &= \text{fluid flow at node 'm', MT}^{-1} \\ q' &= \text{incremental flow unit, MT}^{-1} \\ m &= \text{node number, unitless integer} \end{aligned}$$

For the case illustrated in Figure 3.2.4, n was five and q' was q/15, the uppermost node was numbered one, the middle node was numbered three and the lowest node was number five. The nodal flows are then:

$$q_1 = 1 \cdot q' = q/15,$$

$$\begin{aligned}
q_2 &= 2 \cdot q' = 2q/15, \\
q_3 &= 3 \cdot q' = q/5, \\
q_4 &= 4 \cdot q' = 4q/15, \text{ and} \\
q_5 &= 5 \cdot q' = q/3.
\end{aligned}$$

A 25-cm spatial discretization and a 10-min. temporal discretization were again employed. Radial co-ordinates were simulated by increasing the node and element thicknesses as a function of the lateral distance from the well (Equation 3.2.5).

$$t = 2 \cdot \pi \cdot (X + R_w) \tag{3.2.5}$$

where:

$$\begin{aligned}
t &= \text{node thickness, L} \\
X &= \text{lateral distance from node to well, L} \\
R_w &= \text{well radius, L}
\end{aligned}$$

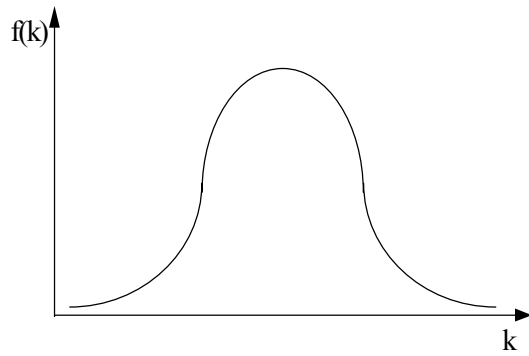
A well radius,  $R_w$ , of 0.61 m (2 ft.) was used in these simulations to approximate the dimensions of the concrete manhole sections commonly used for vertical injection.

#### 3.2.4.1 Vertical Well Model Calibration

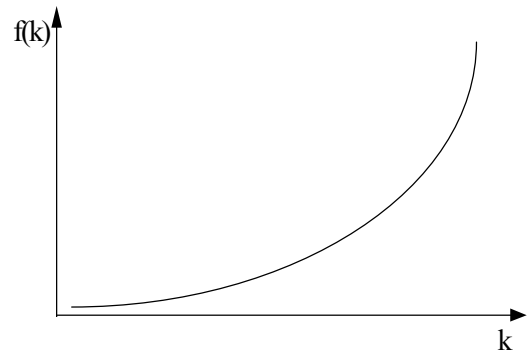
The stability of the vertical well simulations would obviously be impacted by the same factors as the trench simulations. The radial co-ordinates and irregular shape of the saturation profiles made it difficult to calculate accurate mass balances from the saturation iso-clines generated by the Surfer program. Instead, the grid volume information produced by Surfer® for each simulation flow rate was compared to ensure mass balance accuracy. Ultimately, it was found that the 1:100 ratio of compressibility to permeability again applied.

### 3.3 Stochastic Modeling

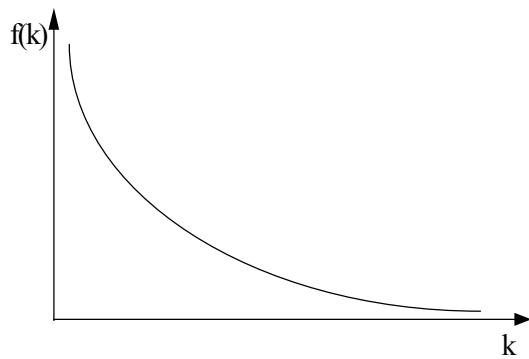
An assessment of the use of stochastic modeling to simulate the heterogeneous nature of solid waste was conducted. The heterogeneities affecting leachate routing were simulated by applying statistical relationships to the permeabilities of the waste mass. Normal, exponentially increasing, exponentially decreasing, and a ‘dog-bone’ probability density functions (PDFs) were used to model the frequency-permeability relationship, Figures 3.3.1a, b, c, and d, respectively.



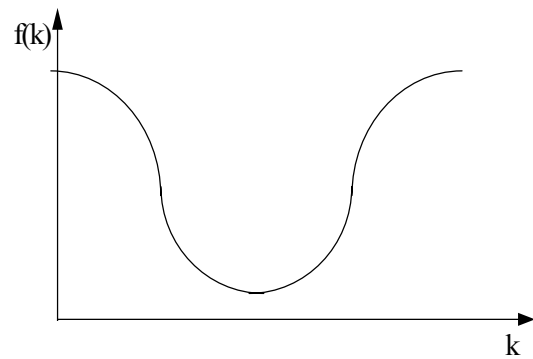
(a) Normal Distribution



(b) Exponential Distribution



(c) Exponential Distribution



(d) Dog-bone Distribution

Figure 3.3.1. Probability density functions used to simulate a heterogeneous waste mass.

Equations 3.3.1a and b were used to plot the normal and exponential probability density functions. The ‘dog-bone’ distribution was based on the theory that the waste mass could have a lot of high and low permeability areas with few median permeability areas and was assumed to have the histogram shown in shown in Figure 3.3.2.

$$f(x) = \frac{1}{\sigma \sqrt{2\pi}} \exp\left[-\left(\frac{x - \mu}{\sigma}\right)^2\right] \quad (3.3.1a)$$

where:

$$\begin{aligned} x &= \text{any value} \\ \sigma &= \text{standard deviation} \\ \mu &= \text{population mean} \end{aligned}$$

$$f(x; \lambda) = \lambda e^{-\lambda x} \quad (3.3.1b)$$

where:

$$\begin{aligned} x &= \text{any value} \\ \lambda &= \text{inverse of the population average.} \end{aligned}$$

Median permeabilities of  $10^{-3}$  and  $10^{-4}$  cm/s, permeability ranges of  $10^{-1}$  to  $10^{-5}$  cm/s and  $10^{-2}$  to  $10^{-6}$  cm/s respectively, were simulated for each probability distribution. For example, the two permeability assignment scenarios for the ‘dog-bone’ PDF case modeled are shown in Table 3.3.1.

Although there are an infinite number of combinations of local permeabilities which could produce each of these distributions, this research was limited to three sets of random numbers to simulate possible waste matrix characteristics. Thus, each probability density function was simulated using three potential waste matrixes generated

by different random number sets. Leachate was applied intermittently, 8 hours per day, for an average rate of  $4 \text{ m}^3/\text{day}/\text{m}$  of trench.

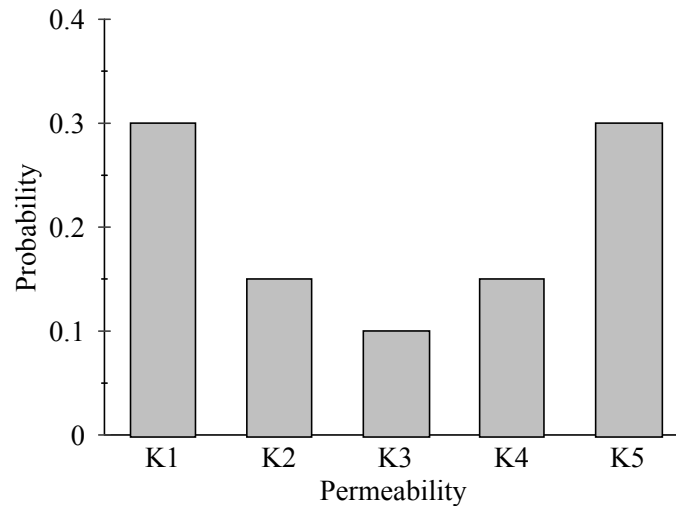


Figure 3.3.2. Histogram used to simulate the ‘dog-bone’ probability distribution

In order to apply the PDFs to the waste mass permeability it was necessary to choose a representative size at which the permeability was constant. It was assumed that the permeability would be constant over a 50 cm by 50 cm cross-sectional zone. The simulation was run using spatial discretizations of 16.6 and 25 cm, breaking each cross-sectional permeability zone into nine and four elements, respectively. Both spatial discretizations resulted in the same saturation iso-clines. Therefore, a spatial discretization of 25 cm was used for the remaining simulations.

Table 3.3.1. Permeability assignments for the two ‘dog-bone’ PDF scenarios modeled.

|                 | Permeability, cm/s |              |
|-----------------|--------------------|--------------|
|                 | Scenario One       | Scenario Two |
| Median          | $10^{-3}$          | $10^{-4}$    |
| K1 <sup>a</sup> | $10^{-1}$          | $10^{-2}$    |
| K2 <sup>a</sup> | $10^{-2}$          | $10^{-3}$    |
| K3 <sup>a</sup> | $10^{-3}$          | $10^{-4}$    |
| K4 <sup>a</sup> | $10^{-4}$          | $10^{-5}$    |
| K5 <sup>a</sup> | $10^{-5}$          | $10^{-6}$    |

<sup>a</sup>refer to Figure 3.3.2.

### 3.3.1 Stochastic Model Calibration

Compressibility again had an impact on the simulation mass balances. The application of the different PDFs to the permeabilities necessitated that a compressibility be determined for each individual PDF. Each simulation was run using a range of compressibilities in order to determine the best compressibility. A mass balance error of <10% was considered acceptable. Based on this constraint, it was impossible to calibrate the

‘dog-bone’ PDF. Results for the normal and exponential PDFs are presented in the results section.

### 3.4 Verificational Modeling

Mathematical modeling is an extremely useful tool which allows parameters to be varied without the expense of physical experimentation. However, without field verification, the validity of model results is questionable. Data were collected from four full-scale sites operating leachate recirculation systems, the Mill Seat Landfill in New York, the Delaware Solid Waste Authority’s Leachate Recirculation Test Cells, the Yolo County Controlled Landfill Demonstration Project in California, and a leachate recirculation test cell constructed by the University of Central Florida in conjunction with the EPA at the Orange County Landfill in Florida. The data were first analyzed for applicability and usefulness. Then, the site recirculation system and operational procedures were modeled in an attempt to verify model estimations. A description of these sites and the accompanying modeling effort follows.

#### 3.4.1 Mill Seat Landfill, Monroe County, New York.



The goal of this project was to design, construct and operate a functional leachate recirculation and gas collection system and demonstrate the feasibility of enhancing methane gas production at an operating landfill. The project is being conducted at the newly constructed Mill Seat Landfill, Monroe County, NY. Monroe County is located in western NY on the southern shore of Lake Ontario.

The project consists of three hydraulically separated cells, a 3-hectare (7.6-ac) control cell (gas collection only), a 2.8 ha (6.9 ac) cell recirculating leachate through pressurized loops, and a 2.2 ha (5.4 ac) cell recirculating leachate through deep horizontal trenches. The pressurized loop system consists of three pressurized loops constructed from a 10-cm (4-in) perforated pipe installed in trenches filled with highly permeable materials such as crushed cullet and tire chips. The loops have been installed at different elevations to enhance wetting. The deep trench system consists of two trenches (1.3 m (4 ft) wide by 3 m (10 ft) deep) filled with permeable wastes. These trenches have been topped with prefabricated infiltrators to enhance drainage. The trenches are fed by tanker trucks which discharge into chimneys constructed through the waste layers above the trench.

Both the pressure loop system and the deep trench were modeled in half-width based on the results from the horizontal trench modeling effort. Diagrams of both system cross-sections are shown in Figure 3.4.1.

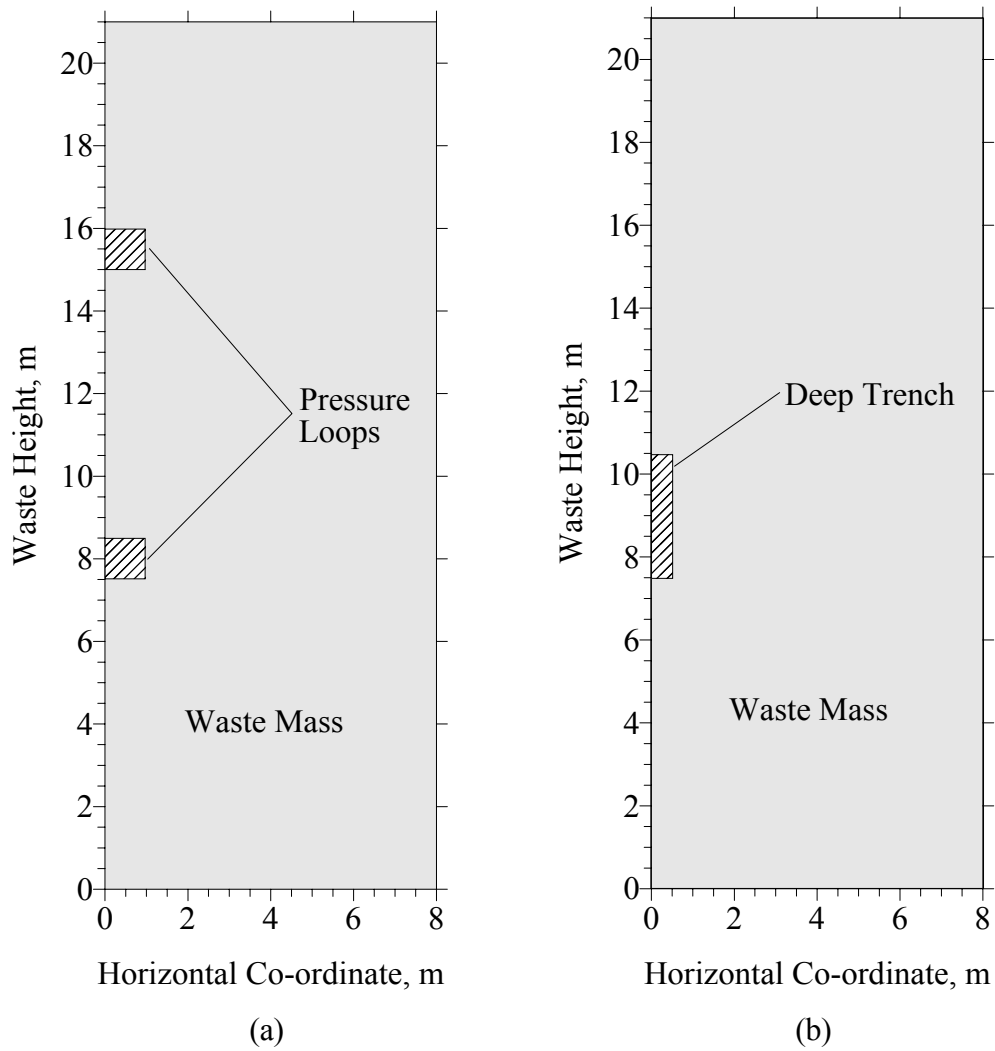


Figure 3.4.1. Schematic diagram of the cross-sections modeled for the pressure loop (a) and deep trench (b) recirculation systems.

Leachate routing was to be monitored via gypsum blocks installed at three elevations within the fill at leachate mass balances. However, the blocks were prematurely wetted during filling and never produced data. Mass balances have been collected for all three test cells and will be used to validate fluid budgets generated during the modeling process.

The cumulative volumes recirculated and generated for the pressure loop and deep trench recirculation systems are shown in Figures 3.4.2 and 3.4.3, respectively.

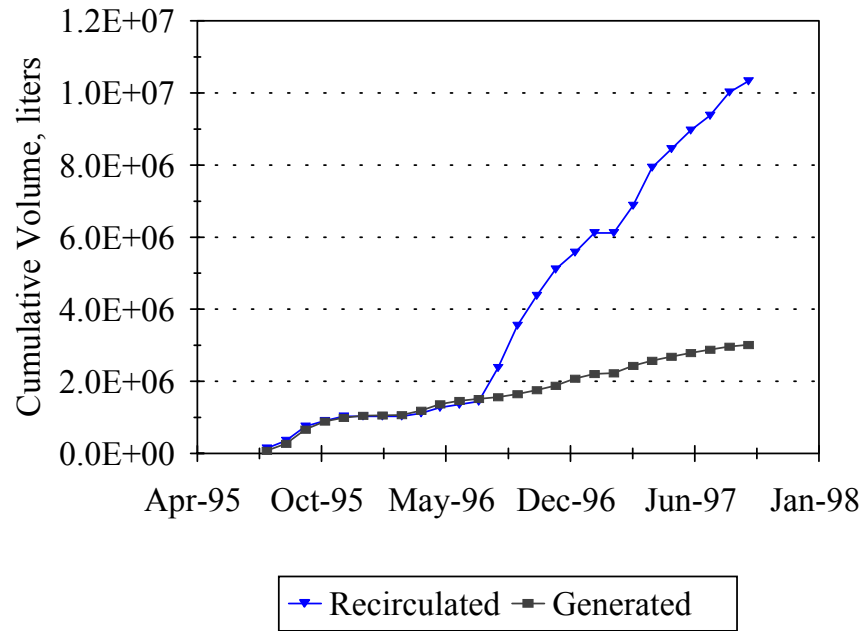


Figure 3.4.2. Cumulative leachate volumes generated and recirculated for the pressure loop recirculation system.

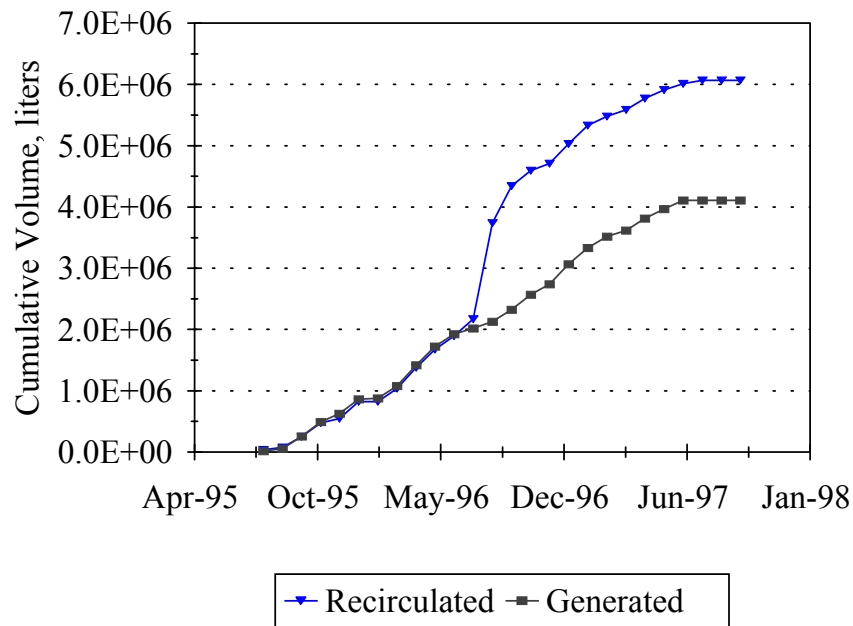


Figure 3.4.3. Cumulative leachate volumes generated and recirculated for the deep trench recirculation system.

### 3.4.2 Delaware Solid Waste Authority.

The DSWA's leachate recirculation test cell has the shape of a truncated pyramid with approximate dimensions as follows, a base area of 3948 m<sup>2</sup> (42,471 ft<sup>2</sup>), an upper area of 921 m<sup>2</sup> (9910 ft<sup>2</sup>), and a waste depth of 7.6 m (25 ft). A 9.45 m by 13.4 m (31 ft by 44 ft) leach field with four separate, but identical, quadrants was constructed just beneath the final cover. Figure 3.4.4. presents historic leachate generation and application information for this site.

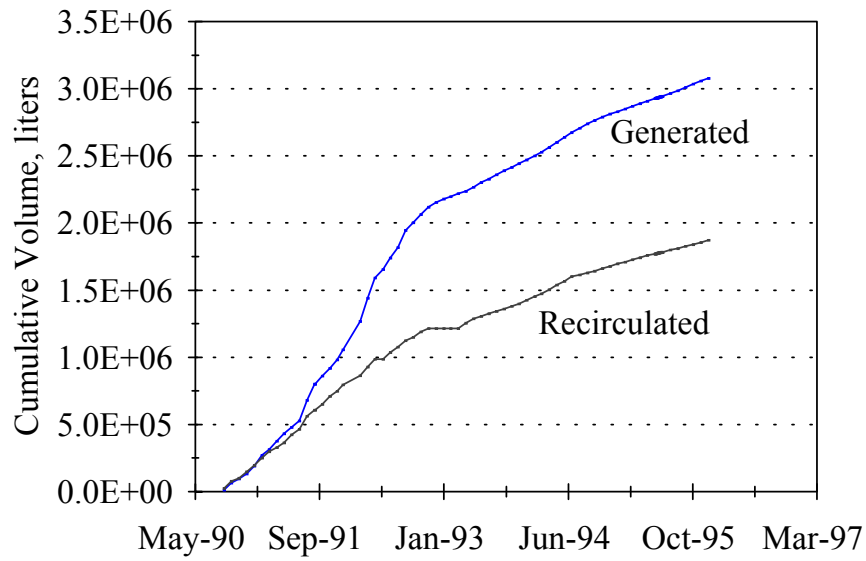


Figure 3.4.4. Cumulative leachate volumes generated and recirculated for the DSWA's leachate recirculation test cell.

The simulation effort modeled one of these quadrants or one-quarter of the test cell. In order to accurately represent this non-symmetrical shape, the quasi-3 dimensional abilities of SUTRA were used. This approach involved specifying lateral thicknesses; essentially a 'z' co-ordinate for each x, y co-ordinate (Figure 3.4.5).

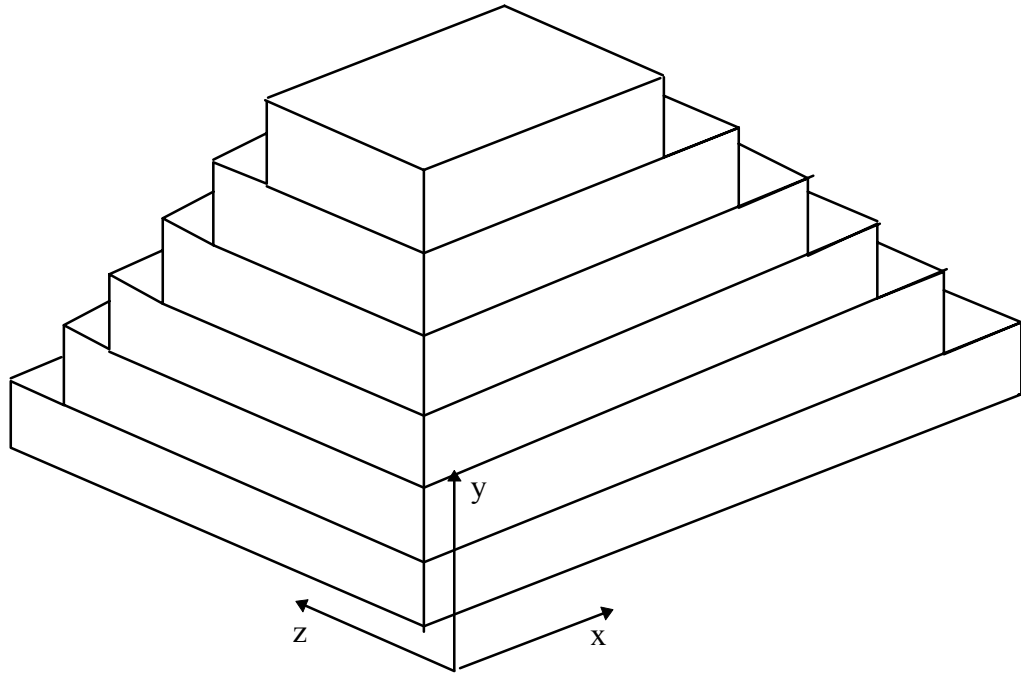


Figure 3.4.5. Co-ordinate Schematic for the DSWA Test Cell Simulations.

The difficulty encountered with this techniques was that SUTRA simulates liquid movement as if it is occurring across the entire thickness ( $z$  co-ordinate) specified. This approach results in the implied assumption that the lateral movement of leachate in the 'z' direction was equal to the local thickness. An iterative approach to calibrating the local thicknesses was then conducted based on the assumption that lateral spreading in the 'z' direction would be approximately equal to lateral spreading in the 'x' direction. Lateral spreading in the 'x' direction could be determined by examining the saturation iso-clines output by the model. A series of simulations were then run where the 'z' co-

ordinates were reduced until the local ‘z’ co-ordinate was approximately equal to leachate spreading in the ‘x’ direction at that point. Modeling time was optimized by reducing the simulation width (x-coordinate) from the full-scale width of 32 m. Those nodes which were significantly beyond the leachate movement in the ‘x’ direction were removed.

The iterative process only required two steps to reach convergence between the leachate movement in the ‘x’ and ‘z’ direction. Table 3.4.1 presents general information on the co-ordinates used in these simulations. The reduced scale simulation number two was used to generate the data presented in the results section.

Table 3.4.1. DSWA test cell simulation lateral boundaries.

| Waste Height<br>(‘y’ co-ordinate),<br>m | Full-scale<br>Simulation |      | Reduced Scale<br>Simulation One |      | Reduced Scale<br>Simulation Two |      |
|---|--------------------------|------|---------------------------------|------|---------------------------------|------|
|   | x, m                     | z, m | x, m                            | z, m | x, m                            | z, m |
| 0                                       | 32                       | 32   | 10                              | 10   | 10                              | 8    |
| 6.75                                    | 6.75                     | 6.75 | 6.75                            | 6    | 6.75                            | 6    |
| 7.5                                     | 6.75                     | 4.8  | 6.75                            | 4.8  | 6.75                            | 4.8  |

The waste mass permeability was initially modeled as  $8.1 \times 10^{-3}$  cm/s based on evaluation of the leachate arrival times. This permeability did not result in the production of leachate as was indicated by the generated data. The permeability was then increased to  $10^{-1}$

cm/s which resulted in better agreement between the generated and simulated leachate production data. A compressibility of  $2 \times 10^{-4} \text{ m} \cdot \text{s}^2 / \text{kg}$  produced good mass balance results for both permeabilities modeled.

### 3.4.3 Yolo County Landfill, California.

The Yolo County LRS Demonstration Project consist of two, 30-m by 30-m (100-ft by 100-ft) cells. Leachate was introduced through a leach field consisting of 14 individual 4-m x 10-m x 1.5-m ( width x length x depth) trenches at the top of one of the 14-m (46-ft) deep cells. The second cell serves as a control with a single composite liner, while the recirculation cell has been constructed with a double composite liner. Independent leachate collection and removal systems were constructed. Pressure transducers located within the LCS monitor hydraulic head. Moisture content is being measured with gypsum moisture blocks and custom PVC/gravel sensors while thermocouples are being used to monitor temperature. Yolo County personnel also plan to measure gas pressure and gas and leachate flow and composition.

Initially, it was envisioned that this system would be analyzed using a cross-section similar to the horizontal trench simulations previously discussed and that actual versus predicted local saturations would be compared. However, the layout of this system made it extremely difficult to isolate a cross-section which could be modeled in this manner. The trenches were more like elongated pits, with approximate dimensions



of 1 m wide by 3.3 m long by 2.6 m deep, than the long line source trench modeled in the conceptual simulations study. The exact dimension and orientation of the trenches varied based on local conditions including waste composition and slope of the landfill surface. The areal layout of the system made the isolation of an individual trench impossible as can be seen in Figure 3.4.6.

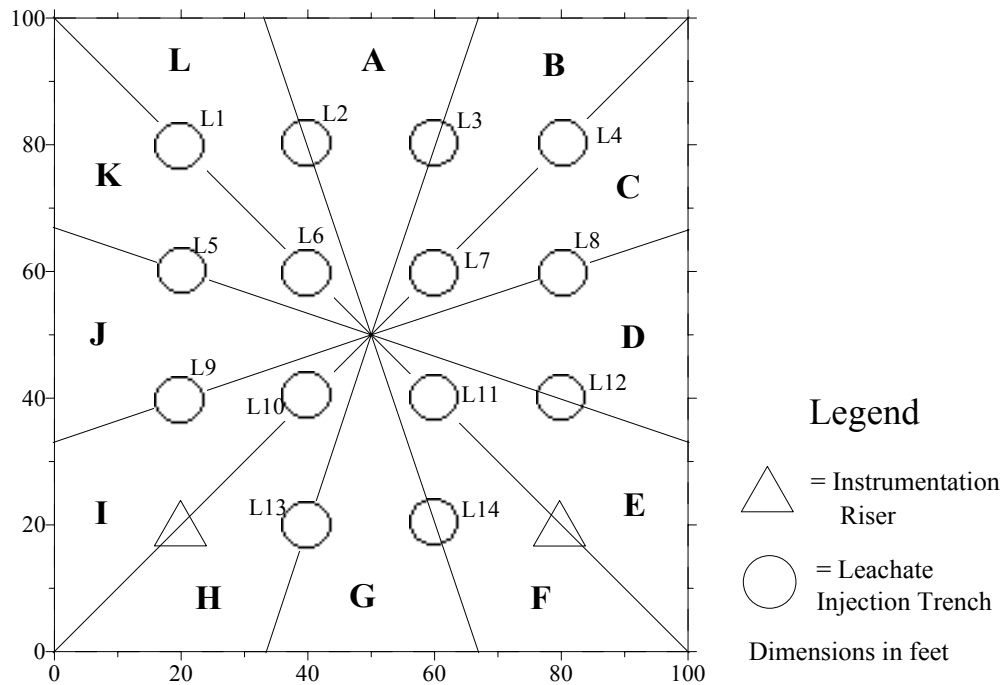


Figure 3.4.6. Areal diagram of the Yolo County leachate recirculation test cell.

Furthermore, the calibration curve required to convert the reading from the gypsum moisture blocks to a moisture content was not developed while the PVC/gravel moisture

sensors were only calibrated for three readings, below field capacity, between field capacity and saturation, and saturated. Thus the information produced by these instruments was more qualitative than quantitative. Yolo County personnel are presently trying to combine leachate mass balance information with the measurements from the gypsum blocks and PVC/gravel sensors to develop calibration curves. Therefore, the system was analyzed by comparing actual and predicted mass balances on leachate arrival and storage rather than for specific local moisture contents.

The areal layout of the system still complicated the development of the finite element mesh. Liquid injections in SUTRA occur across the entire thickness of a node not at a discrete point. Therefore, it was decided to model one section of the areal cross-section with radial co-ordinates. The areal surface was broken into 12 individual sections labeled 'A' through 'L' in Figure 3.4.6. Some of the sections were identical based on geometry and location of injection trenches. The similar sections were found to be

- $A = D = G = J,$
- $L = C,$
- $K = B,$
- $I = F,$  and
- $H = E.$

Section 'A' was ultimately chosen for simulation based on the location of the input devices. Since both devices were located 9.6 m from the center of the landfill, the line source assumption imposed by SUTRA would be most reasonable for this section. All of

the other sections had trenches at various distances from the center of the landfill along both sides of the section. For instance, in section 'K' there are two trenches along one edge at distances of 4.3 m and 12.9 m from the landfill center and one trench along the other edge at a distance of 9.6 m from the center of the landfill. A true three-dimensional modeling effort would be required to fully capture the behavior of this system. The finite-element mesh for the waste mass was constructed using a 50 cm spatial discretization while varying the nodal thicknesses as a function of the distance from the center of the landfill. The increase in the spatial discretization was necessary to conserve simulation time since the overall mass budget was to be evaluated rather than local saturations.

The initial dry-basis moisture content of the system was assumed by the operators to be 25%. This moisture content corresponds to a saturation of approximately 12% based on a porosity of 0.55 and a solids density of  $0.594 \text{ g/cm}^3$  (Moore et al. 1997). Initially, the simulation was started using a saturation of 10%. A waste permeability of  $10^{-1} \text{ cm/s}$  and a compressibility of  $2 \times 10^{-4} \text{ m} \cdot \text{s}^2/\text{kg}$  were used based on the DSWA simulation results and the nearly instantaneous leachate arrival reported. However, the model was very unstable at this saturation and the mass balances could not be calibrated. The first 34 days of operation were then remodeled using initial saturations of 20, 30, and 40 percent with all other inputs held constant including, the waste permeability ( $10^{-1} \text{ cm/s}$ ) and the compressibility ( $2 \times 10^{-4} \text{ m} \cdot \text{s}^2/\text{kg}$ ). These simulations yielded the mass balance results shown in Table 3.4.2.

Table 3.4.2. Simulation mass balance results for initial saturations of 20, 30, and 40 percent after 34 days.

| Initial Saturation, % | Leachate Generated, l | Leachate Stored, l | Total, l | Ratio of Leachate Generated to Leachate Input, % | Error in Mass Balance, % |
|-----------------------|-----------------------|--------------------|----------|--|--------------------------|
| 20                    | 0                     | 49,541             | 49,541   | 0  | 1.2                      |
| 30                    | 204                   | 39,875             | 40,079   | 0.51   | 18.1                     |
| 40                    | 19,349                | 31,868             | 51,217   | 40   | 4.4                      |

Based on the results shown in Table 3.4.2, it was decided that an initial saturation of 40% provided the best combination of simulation mass balance accuracy and prediction of leachate arrival. Yolo County reports indicated that 17% of the applied leachate reached the LCS during the first 34 days of operation. This 17% was generated almost immediately following leachate application.

#### 3.4.4 UCF/EPA Test Cell, Orange County Landfill, Florida.

A test cell was constructed at the Orange County Landfill, Orlando, FL with the specific goal of monitoring leachate flow characteristics. The test cell was constructed during the period of July 1995 to January 1996 in the southwest corner of the Orange County Landfill. The cell had a 4047 m<sup>2</sup> (1 acre) footprint, a maximum depth of 7.3 m (24 ft), and a LCS consisting of a HDPE geo-membrane, geonet, perforated pipe, gravel, and sand. Leachate recirculation was accomplished via a 2-m (6-ft) wide by 9.1-m (30-ft) long by 0.6-m (2-ft) deep trench at the top of the cell. The trench was filled with whole waste tires, gravel, and a perforated PVC pipe which was fed via a multiple-stage centrifugal pump at the landfill leachate sump. Leachate routing was monitored with 48 gypsum blocks installed at various heights within the cell (Figure 3.4.7) and fluid mass balances on both sides of the trench. Soil tensiometers were also installed at the surface of the landfill but yielded little valuable data.

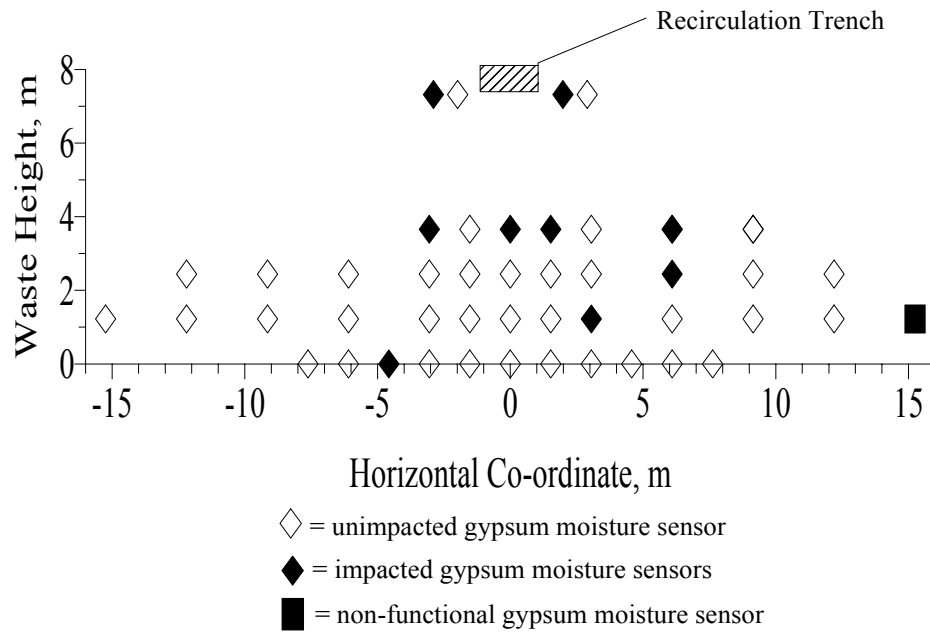


Figure 3.4.7. Location of gypsum moisture sensors used in the UCF/EPA test cell.

The daily cover (silty-sand) applied to the cell eroded into the trench on several occasions and severely impeded leachate flow. The trench was drained and the sides were reinforced with sandbags. Pumping was resumed once the repairs were completed and the trench began to drain again. Nine of the 47 operational moisture blocks (one was damaged during filling operations) generated moisture data during this time period however, no leachate emanated from the LCS.

During the 13 week period from March third to June second, 3,434 l (13,000 gal) of leachate was recirculated. Table 3.4.3. shows the exact times and volumes of leachate application.

The UCF/EPA test cell was modeled using the same dimensional similarity assumption as the trench simulations, i.e. one half of the cross section was monitored (Figure 3.2.1). It was also decided that the waste mass would be modeled as homogeneous with a spatial discretization of 25 cm. This was based on ease of modeling and visual analysis of the waste placed. The majority of the waste placed was residential MSW.

Figure 3.4.8 shows the daily and cumulative volume of leachate added to the simulated waste mass. The simulated application rates were based on modeling one-half of a 1-m section of the 9.1-m long trench. On the days leachate was applied, it was applied over a 2-hr period which is similar to the actual pumping periods used.

Figure 3.4.9 provides information on the accuracy of the simulation output. The error in the liquid mass balance was calculated by comparing the amount of leachate applied to the change in leachate storage within the waste mass. The waste mass was modeled at three different permeabilities,  $10^{-1}$ ,  $10^{-2}$ , and  $10^{-3}$  cm/s, with an initial saturation of 20%. The initial saturation was chosen to be 20% based on data produced by the gypsum moisture blocks and qualitative information on the condition of the placed waste. The best compressibility setting was found to be  $10^{-5}$  m $\cdot$ s $^2$ /kg for all permeabilities modeled. Inspection of Figure 3.4.9 indicates that the simulation with the waste permeability set to  $10^{-2}$  cm/s produces the least overall error, less than 20% until week eight and always less than 40%, while a waste permeability of  $10^{-3}$  cm/s produced the most consistent results, the percent error varied little from 40% over the 13 weeks

Table 3.4.3. Leachate application schedule for the UCF/EPA test cell.

| Day | Leachate Applied, gal | Cumulative Leachate Addition, gal |
|-----|-----------------------|-----------------------------------|
| 1   | 340 (90)              | 340 (90)                          |
| 2   | 1306 (345)            | 1646 (435)                        |
| 3   | 1193 (315)            | 2839 (750)                        |
| 4   | 995 (263)             | 3834 (1,013)                      |
| 5   | 896 (237)             | 4730 (1,250)                      |
| 7   | 1200 (317)            | 5930 (1,567)                      |
| 8   | 638 (169)             | 6568 (1,735)                      |
| 11  | 809 (214)             | 7377 (1,949)                      |
| 12  | 800 (211)             | 8177 (2,160)                      |
| 14  | 1188 (314)            | 9365 (2,474)                      |
| 24  | 1433 (379)            | 10798 (2,853)                     |
| 27  | 270 (71)              | 11068 (2,924)                     |
| 40  | 281 (74)              | 11349 (2,998)                     |
| 44  | 586 (155)             | 11935 (3,153)                     |
| 45  | 4 (1)                 | 11939 (3,154)                     |
| 46  | 80 (21)               | 12019 (3,175)                     |
| 56  | 195 (52)              | 12214 (3,227)                     |
| 68  | 240 (63)              | 12454 (3,290)                     |
| 80  | 200 (53)              | 12654 (3,343)                     |
| 84  | 346 (91)              | 13000 (3,434)                     |

simulated. Based on the results shown in Figure 3.4.9, the  $10^{-2}$  waste permeability simulations were chosen for further analysis. The information presented in Figure 3.4.9 is for a 30-minute time step. A 10-minute time step was also tried but did not produce any significant improvement in the mass balance.



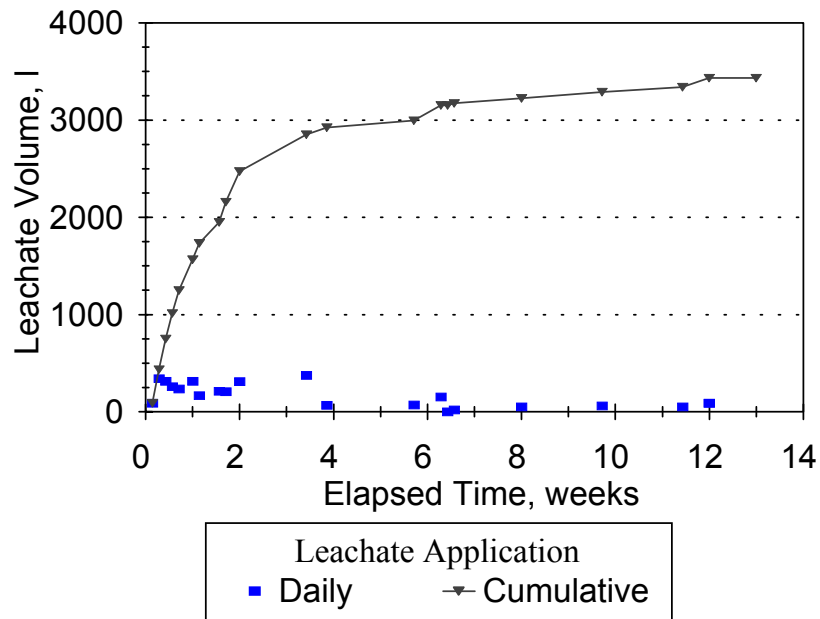


Figure 3.4.8. Daily and cumulative leachate addition to the UCF/EPA test cell.

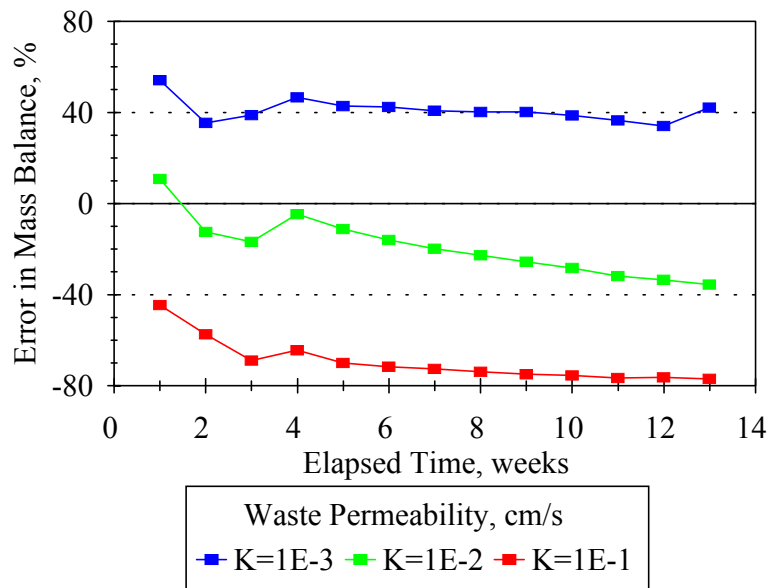


Figure 3.4.9. Percent error between leachate volume stored in waste mass and actual leachate application for the three different waste permeabilities modeled.